

Structure of *Salmonella typhimurium* OMP Synthase in a Complete Substrate Complex

Charles Grubmeyer,^{*,†} Michael Riis Hansen,[‡] Alexander A. Fedorov,[§] and Steven C. Almo^{*,§}

[†]Department of Biochemistry and Fels Research Institute, Temple University School of Medicine, 3307 North Broad Street, Philadelphia, Pennsylvania 19140, United States

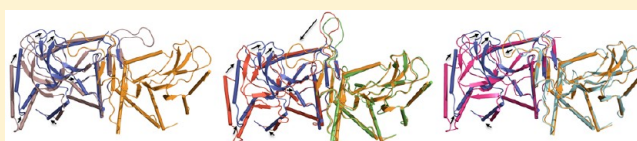
[‡]Department of Biology, University of Copenhagen, Ole Maaløes Vej 5, DK-2200 Copenhagen N, Denmark

[§]Department of Biochemistry, Albert Einstein College of Medicine, 1300 Morris Park Avenue, Bronx, New York 10461, United States

ABSTRACT: Dimeric *Salmonella typhimurium* orotate phosphoribosyltransferase (OMP synthase, EC 2.4.2.10), a key enzyme in de novo pyrimidine nucleotide synthesis, has been cocrystallized in a complete substrate E·MgPRPP-orotate complex and the structure determined to 2.2 Å resolution.

This structure resembles that of *Saccharomyces cerevisiae* OMP

synthase in showing a dramatic and asymmetric reorganization around the active site-bound ligands but shares the same basic topology previously observed in complexes of OMP synthase from *S. typhimurium* and *Escherichia coli*. The catalytic loop (residues 99–109) contributed by subunit A is reorganized to close the active site situated in subunit B and to sequester it from solvent. Furthermore, the overall structure of subunit B is more compact, because of movements of the amino-terminal hood and elements of the core domain. The catalytic loop of subunit B remains open and disordered, and subunit A retains the more relaxed conformation observed in loop-open *S. typhimurium* OMP synthase structures. A non-proline *cis*-peptide formed between Ala71 and Tyr72 is seen in both subunits. The loop-closed catalytic site of subunit B reveals that both the loop and the hood interact directly with the bound pyrophosphate group of PRPP. In contrast to dimagnesium hypoxanthine-guanine phosphoribosyltransferases, OMP synthase contains a single catalytic Mg²⁺ in the closed active site. The remaining pyrophosphate charges of PRPP are neutralized by interactions with Arg99A, Lys100B, Lys103A, and His105A. The new structure confirms the importance of loop movement in catalysis by OMP synthase and identifies several additional movements that must be accomplished in each catalytic cycle. A catalytic mechanism based on enzymic and substrate-assisted stabilization of the previously documented oxocarbenium transition state structure is proposed.



Orotate phosphoribosyltransferase (OMP synthase, EC 2.4.2.10) catalyzes the formation of the nucleosidic bond in de novo pyrimidine nucleotide synthesis. Orotate and the ribosyl 5-phosphate donor PRPP react with the loss of pyrophosphate to form OMP, the precursor to UTP. OMP synthase is a discrete protein in bacteria and fungi. In higher eukaryotes, this activity is part of the bifunctional UMP synthase (OMP synthase, OMP decarboxylase),¹ the locus for hereditary orotic aciduria.² The enzyme is one of 10 phosphoribosyltransferases (PRTases) characterized by their base specificity.³ The PRTase group is now known to contain several distinct evolutionary families, based on different architectures. The Rossmann fold-based Type I PRTases constitute the enzymes of de novo and salvage purine and pyrimidine biosynthesis, including hypoxanthine-guanine PRTase (HGPRTase), GPAT, adenine PRTase, OMP synthase, and uracil PRTase.⁴ The Type I PRTases show minimal sequence conservation among different substrate specificity classes, mainly centered on a short PRPP binding motif.⁵ More widespread conservation of sequence is observed among enzymes for each substrate class. PRPP synthase, in which the β - γ pyrophosphoryl group of ATP reacts with O1 of ribose 5-phosphate, also exhibits the Type I fold.⁶ The Type II enzymes, of TIM barrel architecture, are represented by

pyridine PRTase, including quinolinate PRTase,⁷ nicotinate PRTase,⁸ and nicotinamide PRTase.⁹

The paradigm for the Type I enzymes has been HGPRTase, exemplified by the human¹⁰ and bacterial¹¹ enzymes as well as enzymes from the eukaryotic parasites *Trichomonas foetus*,¹² *Plasmodium falciparum*,¹³ and *Toxoplasma gondii*,¹⁴ determined in complexes including base, PRPP,¹⁵ and nucleotide.¹⁶ The structure of a complex with a transition state analogue has also been determined¹⁷ and provides a view along the reaction coordinate. A major finding from the HGPRTase structures is that the enzyme can exist in a relatively open form, whose active site, including the bound substrate, is exposed to bulk solvent,¹⁰ which is not compatible with the development of high-energy transition states for group transfer. Active site closure is provided by a disordered loop of the peptide, formed by an extension of the nucleotide fold, which projects into solvent adjacent to the active site. This “flexible loop”, sometimes termed Loop II,¹⁶ adopts a folded and ordered β -structure in transition state analogue complexes, and several residues from the loop project into the active site. In the loop-

Received: January 18, 2012

Revised: April 24, 2012

Published: April 24, 2012



closed complexes, active site water molecules are highly ordered, with low *B* factors, and are positioned away from the developing oxocarbenium ion. In each catalytic cycle, the flexible loop needs to move between its open position to a closed position to interact with bound ligands.^{17,18} Other Type I PRTases contain a homologue of the flexible loop. Motional studies have been conducted on the GPAT loop,¹⁹ and in that case, X-ray diffraction studies have captured the loop in open and closed positions.

As seen with HGPRTases, the catalytic loop of OMP synthase (residues 99–109 in the *Salmonella typhimurium* enzyme) adopts an open and disordered conformation in X-ray structures of E-OMP and E-MgPRPP-*orotate* complexes.^{20,21} Notably, this dynamic loop exhibits the highest level of sequence conservation of any contiguous region in the protein, indicating significant functional importance. Chemical modification and mutagenesis studies²² have shown that loop residues Lys103 and Lys100 are important for activity. Complementation experiments have demonstrated that Lys103 exercises its catalytic function in the active site formed by the adjacent subunit, while Lys100 acts in the active site formed by its own subunit.²³ A three-dimensional structure of the highly homologous *Escherichia coli* enzyme, in complex with an inhibitory sulfate anion, captured one of the two loops in a more structured “loop-closed” conformation atop the active site of the adjacent subunit.²⁴ In this case, Lys103 formed a hydrogen bond with the sulfate anion, which occupied the position of the β -phosphate of bound PRPP in the earlier structure. A structure of the yeast enzyme has captured a symmetric ternary complex of the enzyme, MgPRPP, and *orotate* in which each loop is closed over the adjacent active site of the dimer.²⁵ The groups of Witte and McClard have also shown that the yeast enzyme demonstrates half-of-the-sites binding, leading to a proposal that the enzyme follows a complex “double Theorell–Chance” mechanism.²⁶ Because the yeast and bacterial enzymes are structurally similar, it quite likely that findings for each have relevance to a general mechanism.

The emerging dynamic picture is that the loop from one subunit moves from a solvent-extended and disordered form to a highly structured one that occludes solvent from the active site of the adjacent subunit. It has been shown that as for HGPRTase, the chemistry of group transfer is rapid, whereas a subsequent step, proposed to be related to loop opening, is rate-determining.²⁷ Nuclear magnetic resonance (NMR) has shown that the catalytic loop of OMP synthase moves between the flexible solvent-extended open position and a closed position. Overall PRPP binding and release from binary complexes is a two-step partitioning process in which the loop moves between open and closed positions and PRPP dissociates from the loop-open complex.²⁸

We have crystallized a complete substrate complex of the enzyme, *orotate*, and MgPRPP. The structure shows one catalytic loop in a stabilized conformation positioned over the ligands in the adjacent subunit, with several residues of the loop forming new contacts to the bound substrate. The major part of the loop from the other subunit extends into the solution and remains disordered.

METHODS

Enzyme. Recombinant *S. typhimurium* OMP synthase was expressed in *E. coli* and purified to homogeneity.²² For crystallization, an ammonium sulfate suspension of the enzyme

was centrifuged and the precipitate dissolved in 20 mM Na-HEPES (pH 7.2). The solution was then repeatedly concentrated on a Centricon-10 (Amicon) and rediluted with the same buffer.

Crystallization. *S. typhimurium* OMP synthase (15 mg/mL, 0.65 mM) was cocrystallized with a 1:0.8 molar stoichiometry of *orotate*, with excess PRPP and MgCl₂ by the hanging drop vapor diffusion method at 18 °C. A 10 μ L drop of 0.1 mM *orotate* was pipetted onto a siliconized cover slide and allowed to dry completely; 2 μ L of a protein solution containing 3 mM PRPP and 6 mM MgCl₂ was placed on top of the dried substrate and mixed with 2 μ L of the reservoir solution. This solution was equilibrated against 700 μ L of reservoir solution composed of 1.4 M trisodium citrate brought to pH 6.5 with HCl. The dimensions of the rectangular crystals were approximately 0.4 mm \times 0.3 mm \times 0.2 mm. Prior to data collection, the crystal was placed in reservoir buffer supplemented with 20% glycerol, 0.006 mM *orotate*, 3 mM PRPP, and 6 mM MgCl₂.

Data Collection and Reduction. X-ray diffraction data were recorded from crystals flash-frozen in a stream of nitrogen at -178 °C, on an image plate detector (Rigaku R-Axis IV) coupled to a rotating-anode X-ray generator (Rigaku RU-H3R) using Cu K α radiation (50 kV and 100 mA). The data were processed using DENZO and SCALEPACK.²⁹ Diffraction from these crystals is consistent with orthorhombic space group C222 with the following cell parameters: *a* = 105.57 Å, *b* = 154.23 Å, and *c* = 52.60 Å. On the basis of the space group symmetry, the unit cell volume, and the molecular mass of 23546 Da, a single dimeric protein molecule per asymmetric unit was proposed (*V*_m of 2.27 Å³/Da and solvent content of 45.47%). The *R*_{sym} on intensities, for 29410 reflections to 2.2 Å resolution (99.9% complete), was 4.7%; 91.3% of the reflections had *I*/ σ (*I*) > 1.0.

Structure Solution and Refinement. The structure was determined by molecular replacement using AmoRe implemented in CCP4³⁰ with the partially closed *E. coli* OMP synthase dimer (97% identical sequence) as the search model.²⁴ The best solution after rigid body refinement gave an *R* factor of 46.6% and a correlation coefficient of 38.3% using 8.0–4.0 Å data. The OMP synthase complex structure was further refined using Xplor,³¹ without inclusion of the catalytic loop residues (102–108). Subsequently, the catalytic loop for subunit A and other smaller loops were built into the electron density map using O.³² The *orotate*, PRPP, Mg²⁺, and water molecules were included in the model, when structural refinement had reached an *R*_{free} of 33.0%. The coordinates of PRPP and *orotate* were taken from the Hetero-Compound Information Center Database,³³ based on a nonproductive base analogue complex with *T. gondii* HGPRTase.³⁴ The ligands were readily identified from significant and well-resolved peaks in the *F*_o – *F*_c map. The 2*F*_o – *F*_c and *F*_o – *F*_c maps showed clear electron density for a *cis*-peptide bond connecting Ala71 and Tyr72 in both subunits. Water molecules were built into 3 σ density in *F*_o – *F*_c maps and retained in the model if the *B* factors refined to below 60 Å². The final model contains 419 residues (102B–108B are not included), two *orotate* molecules, one PRPP molecule, one Mg²⁺ (no PRPP or Mg²⁺ was observed in subunit A), and 384 water molecules with *R*_{work} and *R*_{free} values of 22.5 and 28.9%, respectively. The final model was analyzed with PROCHECK,³⁵ with 91.2% of the residues in the most favored regions, 8.5% in the additional allowed regions, and only Glu163 (A subunit) in the disallowed regions, although this

residue fits well in the electron density map. Details of the data collection and refinement parameters are listed in Table 1. The

Table 1. Data Collection and Refinement Statistics

Data Collection	
data range (Å)	20.0–2.0 (2.07–2.00)
completeness (%)	99.9 (99.1)
R_{sym} (%)	4.7 (37.5)
$I/\sigma(I)$	20.35 (4.23)
mosaicity	0.47
no. of observations	419629
no. of unique reflections	29410
space group	C222
a (Å)	105.57
b (Å)	154.23
c (Å)	52.60
Refinement	
missing residues 102–108 in the B monomer	
resolution range (Å)	8.0–2.2
σ cutoff applied	$2\sigma(F)$
no. of unique reflections	24601
R_{work} (90% of the data) (%)	22.5
R_{free} (10% of the data) (%)	28.9
total no. of non-H atoms	3725
no. of protein atoms	3274
no. of other atoms	66
no. of metal atoms	1
no. of water molecules	384
rmsd from ideal geometry	
bond lengths (Å)	0.008
bond angles (deg)	0.944
torsion angles (deg)	13.786
improper angles (deg)	1.544
average B value (Å ²)	
all atoms	29.21
all protein atoms	27.05
main chain atoms	25.31
side chain atoms	28.87
water molecules	44.80
ϕ and ψ map statistics	
most favored regions	91.2%
additional allowed regions	8.5%
disallowed regions	0.3%

catalytic loop of subunit A and the PRPP-orotate complex of subunit B fit well in the 1σ level $2F_o - F_c$ electron density map as shown in panels A and B of Figure 1, respectively.

Figures were made using PyMOL Molecular Graphics System, version 1.3 (Schrödinger, LLC, New York).

RESULTS

General Description of the Structure. The E·MgPRP-P-orotate complex is an asymmetric dimer similar to that observed in previous OMP synthase structures and other members of the PRTase family. The structure of the subunit is shown as a stereo ribbon diagram in Figure 2, and the dimer is shown in Figure 3. The Type I PRTase fold observed in *S. typhimurium* and *E. coli* OMP synthases in previous complexes is followed by the complete substrate complex here. The structure contains an amino terminal β -hairpin “hood” anchored by an α -helix, a Rossmann fold core containing the prominent catalytic loop, and a pair of carboxyl-terminal α -

helices. These structural elements were renumbered here from previous publications²¹ to include the β -strands of the hood. Strikingly, the catalytic loop of subunit A is seen in a previously undescribed conformation atop the active site of subunit B, where it forms a compact β -structure. The dimer interface is very similar to that described previously,^{20,21} and when interface areas of the two subunits are superpositioned, they appear to be nearly identical. The exception to this occurs in the main chains and side chains of Arg99A and Lys100B, which have moved as discussed later. The asymmetry of the catalytic loop and at Arg99 and Lys100 is important for function.

Asymmetry of the Dimer. Previously reported structures of *S. typhimurium* E·OMP [Protein Data Bank (PDB) entry 1STO] and E·MgPRPP-orotate (PDB entry 1OPR) complexes were fully symmetric.^{20,21} The SO_4^{2-} -bound complex of the *E. coli* enzyme (PDB entry 1ORO) was asymmetric with one of the catalytic loops disposed toward the catalytic site of the adjacent subunit, while the other loop was disordered.²⁴ In the current complex (PDB entry 1LH0), the dimer is highly asymmetric, with movement of the catalytic loop from subunit A and dramatic structural rearrangements of subunit B, yielding an active site more buried than that in the previous sulfate complex. Figure 4 shows overlays of subunits A and B (panel A), the current structure and the more loop-open E·MgPRP-P-orotate structure of Scapin et al.²¹ (panel B), and the current structure and the asymmetric sulfate complex of Henriksen et al.²⁴ (panel C). A few key movements are described here. The hood region ($\text{C}\alpha$ of Lys26B) has moved 5.4 Å toward the subunit interface ($\text{C}\alpha$ of Tyr95B), together with $\alpha 6$ and $\alpha 7$. The segment composed of residues 124–130, and its extension $\alpha 4$ (130–142), shows a 1.6 Å rmsd between the subunit A and B structures. The difference is mainly the result of an upward motion of the backbone at 5-phosphate binding residues 127B–130B, where the side chain of Thr128 forms a new hydrogen bond with the orotate carboxylate. In subunit A, the phosphate-binding residues are comparatively disordered (with poor electron density). Most visibly, the catalytic loop of subunit A has moved 22 Å ($\text{C}\alpha$ of Gly106A of PDB entry 1LH0 vs PDB entry 1OPR²¹) and reordered to the top of the subunit B active site. Lys100 of subunit B extends into the subunit B active site to interact with PRPP. As part of the loop movement, Arg99A makes strong interactions across the subunit interface with PRPP in subunit B that pull the A loop toward subunit B. The loop movement pulls Lys100A away from the PRPP binding site of subunit A. Competition between the two subunits for preferential hydrogen bonding by Arg99 and Lys100 thus may drive the observed asymmetry, as discussed below. It should be noted that in the C222 space group, subunit A and subunit B experience different packing interactions, including close packing around the carboxyl terminus of subunit B. It is not possible a priori to determine whether these crystal packing interactions result from, or help induce, the observed asymmetry.

Structure of the Active Site. The catalytic site of loop-closed subunit B is formed by contributions from the hood, residues at the carboxyl ends of $\beta 3$, $\beta 4$, $\beta 6$, and $\beta 7$, and residues from the catalytic loop of subunit A. The hood forms a cover to the base-binding site in the structures of all complexes determined to date.^{20,21,24} The ϵ -amino group of Lys26B interacts with the pyrophosphate O1A atom of PRPP (3.2 Å) and with the carboxylate of Glu135B in $\alpha 4$ (2.8 Å; this distance is 9.0 Å in subunit A) (Figure 5). The main chain oxygen and nitrogen of Phe35B interact with bound orotate, which also

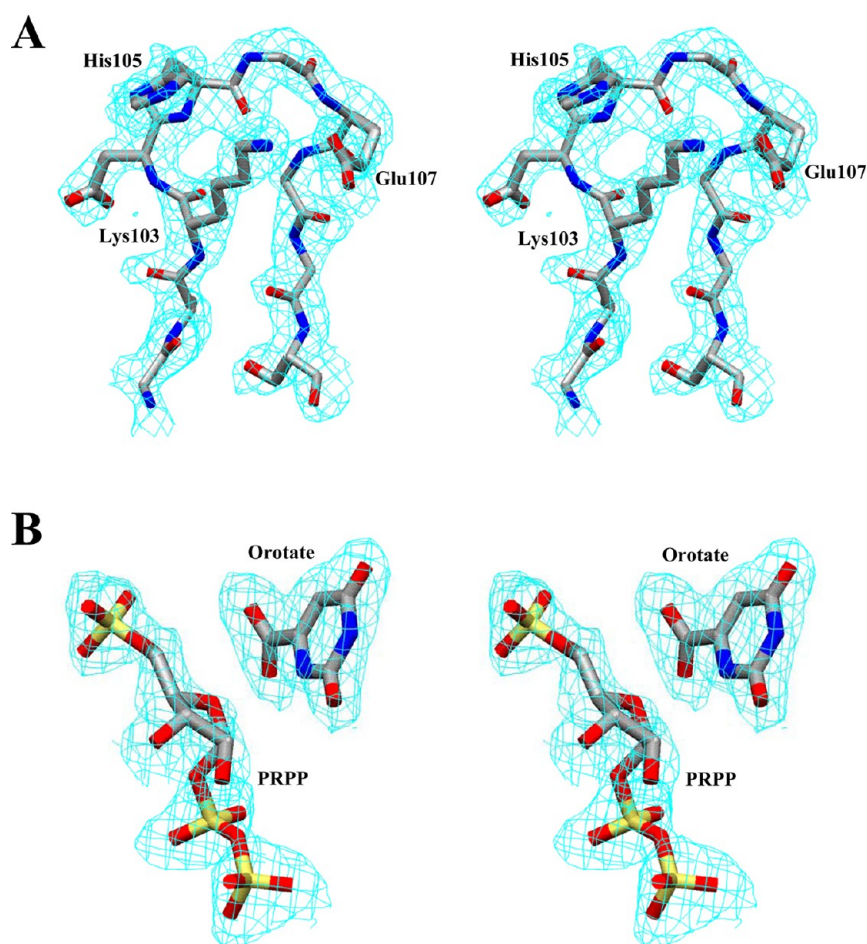


Figure 1. Stereoview of the $2F_o - F_c$ electron density map at 1σ for the structural model of (A) the catalytic loop of subunit A and (B) bound PRPP and orotate in subunit B.

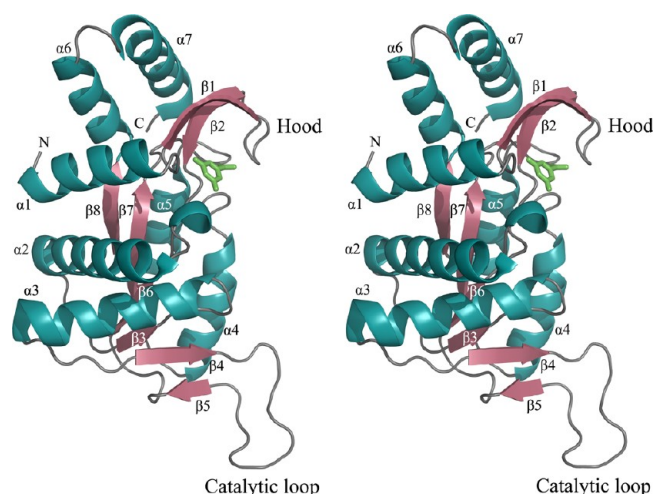


Figure 2. Stereo ribbon diagram of subunit A of the OMP synthase complex. Orotate is colored green.

stacks against the side chain of Phe34B in the hood domain. The guanidino group of Arg156B from the end of $\beta 7$ interacts with the O4 atom of orotate (2.8 Å). The conserved PRPP binding motif⁵ extends from position 120 to 132, which encompasses $\beta 6$ and its extension into a tight loop. The top of $\beta 6$ provides Asp124B, whose carboxyl interacts with O3' of PRPP (2.7 Å), and Asp125B, whose carboxyl is near O2' of

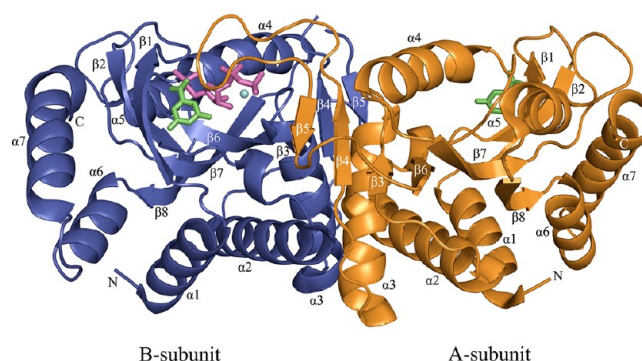


Figure 3. Ribbon diagram of the dimeric OMP synthase complex. Orotate (green), PRPP (magenta), and Mg^{2+} (cyan) are drawn as ball-and-stick models. No PRPP or Mg^{2+} was observed in subunit A. Subunit A is colored orange and subunit B blue.

PRPP and O2 of orotate (Figure 5). The highly conserved residues Thr128B, Ala129B, Gly130B, Thr131B, and Ala132B provide interactions via their amide nitrogens and the side chain hydroxyls with the 5-phosphate of PRPP. The main chain nitrogens of Tyr72B and Lys73B in $\beta 3$ project into the active site where they interact with O3B of the pyrophosphate of PRPP. Residues from $\beta 4$ and the catalytic loop provide interactions with the bound pyrophosphate group of PRPP through the guanidino nitrogens of Arg99A, the ϵ -amino of

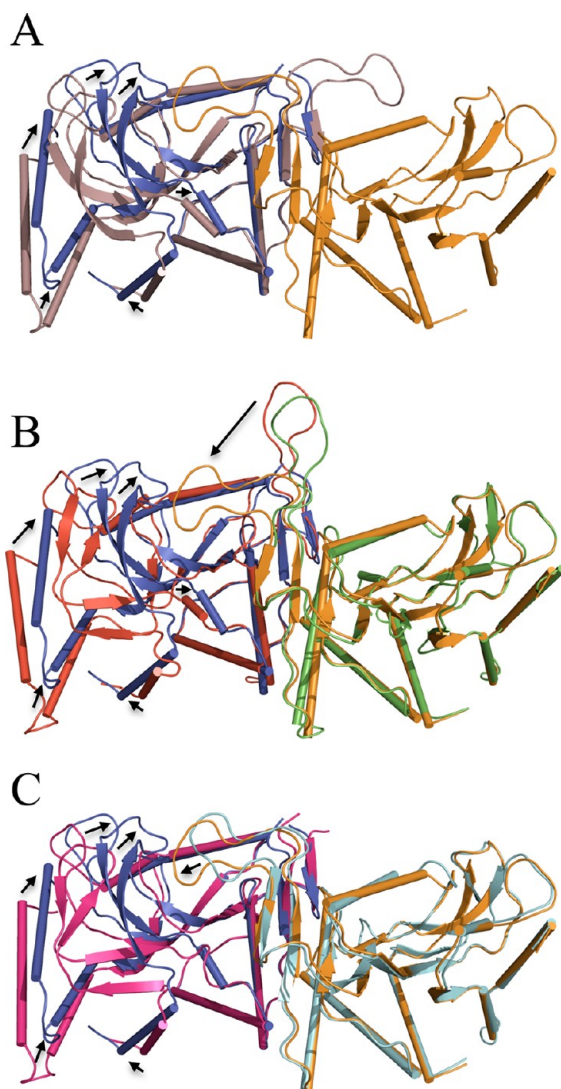


Figure 4. Superposition of OMP synthase structures. (A) Subunit A of the current structure (PDB entry 1LH0, violet) is overlaid on subunit B of PDB entry 1LH0 (blue) of the dimer on the left side, and subunit A is shown on the right side and colored orange. (B) The two subunits (red and green) of the previous loop-open E-MgPRPP-ornate dimer (PDB entry 1OPR²¹) are overlaid on the current complex (PDB entry 1LH0, blue and orange). (C) The two subunits of the sulfate complex colored pink and cyan (PDB entry 1ORO²³) are overlaid on the current structure (PDB entry 1LH0) colored blue and orange. In each panel, residues of the interface were used for superpositioning. Black arrows show major movements. Ligands are not shown.

Lys100B, the ϵ -amino of Lys103A, and the ϵ -imino nitrogen of His105A.

The non-proline *cis*-peptide bond between Ala71 and Tyr72 is unusual. In OMP synthase, the previous PRPP and ornate complex contained a *trans*-peptide bond at this position, although the sulfate complex showed the *cis*-peptide bond. HGPRTase has a non-proline *cis*-peptide at its homologous position.¹⁴

Structure of the Catalytic Loop. The catalytic loop of subunit A lies tightly against the active site formed by subunit B. The loop in this conformation exhibits β -strand-like geometry over much of its length, with residues 104A–108A forming a hydrogen-bonded turn (Figure 1A). There are three ~ 3 Å backbone hydrogen bonds that are internal to the loop: N

Lys103A–O Gly109A, N His105A–O Lys103A, and N Gly108A–O His105A. Two additional intraloop bonds involve side chain nitrogens of Lys103A and Arg99A and O ϵ of Glu107A. The loop also interacts with the hood through N Gly106A forming a 2.8 Å hydrogen bond to the main chain carbonyl oxygen of Thr24B. In addition, hydrogen bonds form between the loop and bound ligands: the ϵ -amino group of Lys103A forms hydrogen bonds to the α - β bridging O3A atom (2.8 Å) and β -phosphate O1B atom (3.1 Å), and the N ϵ atom of His105A forms a hydrogen bond (2.7 Å) to the α -phosphate O2A atom. All these interactions contribute to the stabilization of the closed conformation.

Orotate Binding. Orotate binding is similar in the two subunits of the 1LH0 complex, but somewhat different in detail from that reported previously.²¹ In loop-closed subunit B, orotate is bound by residues Lys26B and Phe35B contributed by the hood, Arg156B from β 7, and Thr128B from the phosphate-binding loop formed by the extension of β 6. Bound orotate forms a stacking interaction with the side chain of Phe34B (see Figure 5). N1 of orotate is 3.7 Å from C1' of PRPP, its site for nucleophilic attack, and is close (3.9 Å) to O4' of PRPP. For formation of a bond between N1 of orotate and C1' of PRPP to occur, N1 must be in a deprotonated state. Figure 5 shows bound orotate in its N1 lactim, with O2 as the deprotonated enolate. This dianionic form of the base has been documented through transition state analysis of the *S. typhimurium*, human, and *Plasmodium* OMP synthases.^{36,37} The N1–O2 lactam could also be accommodated by the X-ray data. Two bound water molecules, w3020 and w3001, form interactions with O2 and may be involved in its deprotonation. The yeast OMP synthase shows two similarly positioned water molecules, and the authors propose their catalytic role in deprotonation from the neutral O2 enol lactim.²⁵ In PDB entry 1LH0, N3 of orotate interacts with the main chain carboxyl oxygen of Phe35B (2.7 Å), as observed previously.²¹ O4 of orotate forms H-bonds from the main chain nitrogen of Phe35B and the guanidino nitrogen of Arg156B. The carboxylate of orotate is known to be a major contributor to base specificity.^{22,38} One of the carboxylate oxygens is close (3.5 Å) to O4' of PRPP, which may enhance oxocarbenium ion formation. The same orotate carboxylate atom forms a hydrogen bond (2.8 Å) to the main chain nitrogen of Lys26B and to one water molecule [w3017 (2.9 Å)]. The other carboxylate oxygen interacts with the side chain oxygen of Thr128B (2.6 Å) and a water molecule [w3002 (2.7 Å)].

In subunit A, the active site is more loop-open and the bound orotate molecule makes similar but fewer interactions. The major difference in orotate binding between the two subunits is the hydrogen bond to Thr128 present in subunit B. The latter hydrogen bond may be a critical determinant of the compact nature of subunit B, pulling the phosphate binding loop, and PRPP, toward the hood.

MgPRPP Binding. OMP synthase and GPAT³⁹ are distinct among Type I PRTases in having a single Mg²⁺ ion in the catalytic complex. The OMP synthase Mg²⁺ ion is six-coordinate (Figure 6) with a somewhat distorted octahedral geometry. The Mg²⁺ interacts with O2' (2.5 Å) and O3' (2.6 Å) of the ribosyl group, the pyrophosphate O3B (2.4 Å) and C1'–PP bond-bridging O1 (2.5 Å) atoms of the pyrophosphoryl group, and two water molecules [w3053 (2.5 Å) and w3026 (2.3 Å)]. The Mg²⁺ ion makes no direct interactions with the enzyme. This pattern is similar to that of the first Mg²⁺ in the HGPRTase transition state analogue structure.¹⁷ Disruption of

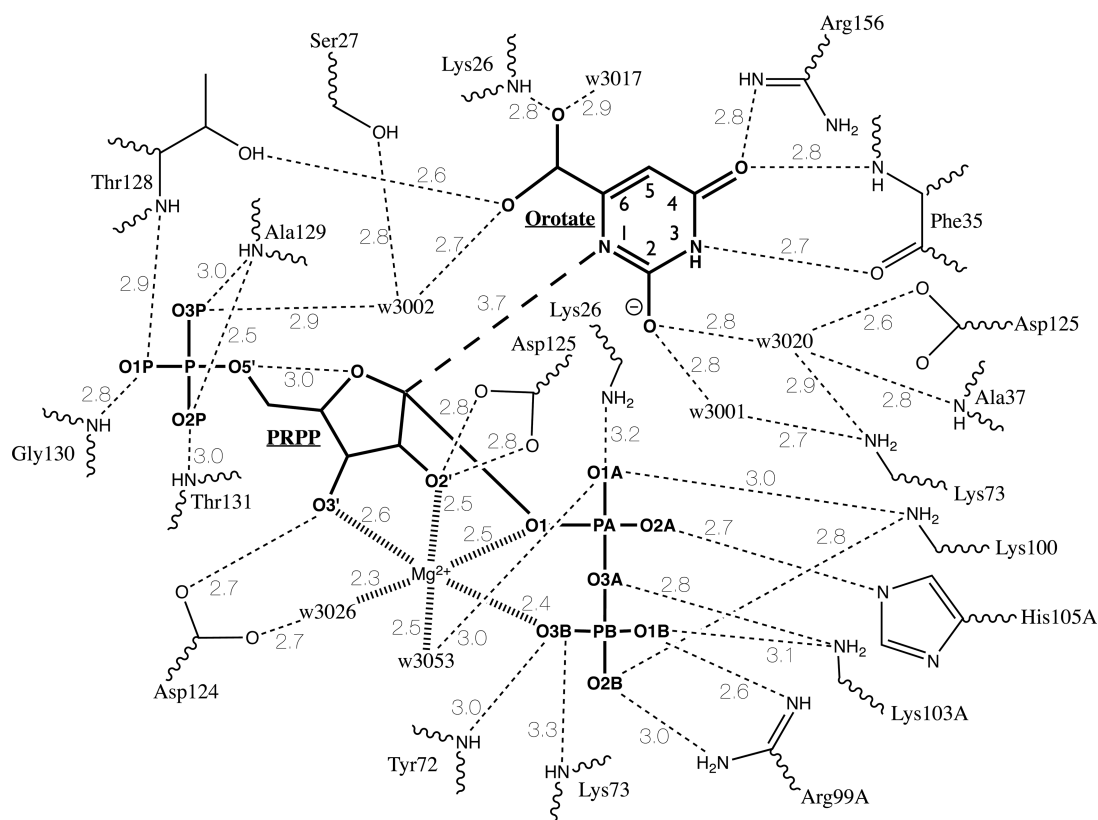


Figure 5. Cartoon of binding interactions in the active site of subunit B. Substrate covalent bonds are shown in bold. Hydrogen bonds (<3.5 Å) are shown as dashed lines. The bold dashed line indicates the N1 (orotate) to C1 (PRPP) reaction coordinate. Mg^{2+} coordination bonds are shown as hashed lines. Solvent water molecules are denoted with a “w” with the four digits of the PDB designation shown. Note that residues Lys26, Lys73, and Asp125 are each shown twice.

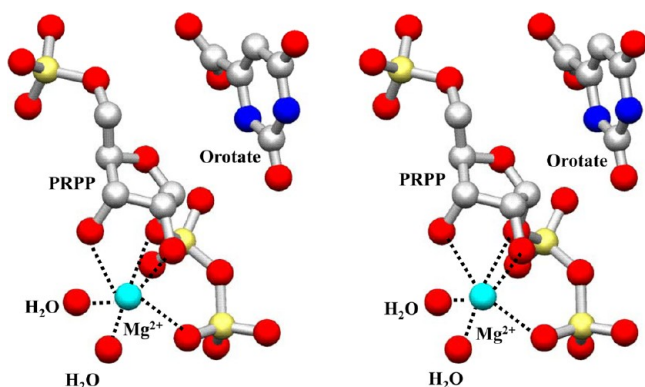


Figure 6. Stereoview of the coordination of the Mg^{2+} ion in subunit B.

the C1'–OPP_i bond may relieve the distortion of coordination seen here. Neutralization of the pyrophosphate charge is accomplished by the positive charges from the catalytic loop (Arg99A, Lys100B, and Lys103A) and the hood (Lys26B). The sugar conformation is difficult to discern unambiguously at 2.2 Å resolution; however, the refined PRPP is consistent with the furanose conformation reported in the *T. gondii* HGPRTase-MgPRPP structure³⁴ that served as the starting point for the refinement.

The 5-phosphate group of PRPP is remarkable in that every oxygen participates in multiple hydrogen bonds that firmly anchor the group to the main chain N atoms of residues of the 5-phosphate-binding loop [Thr128B–Gly132B (Figure 5)]. The hydrogen bond network serves to position OS' within 3.0

Å of the ribosyl ring oxygen. Sugar atoms O2' and O3' interact with residues Asp125B (O2'; two 2.8 Å bonds) and Asp124B (O3'; 2.7 Å bond) and one water molecule [w3001, O3'; 3.0 Å bond (this interaction is not shown in Figure 5)].

In subunit B, the pyrophosphoryl group of PRPP interacts to form a strikingly extensive and tight hydrogen bond network with residues from both catalytic loops, the hood, the $\beta 3$ – $\alpha 3$ turn, bound Mg^{2+} , and several waters. The catalytic loop of subunit B contributes Lys100B, whose ϵ -amino group forms hydrogen bonds to α - and β -phosphate. Subunit A provides Arg99A, which forms two bonds with β -phosphate. The catalytic loop of subunit A also provides Lys103A, which forms hydrogen bonds to α - and β -phosphate, and His105A, whose ϵ -imino nitrogen interacts with α -phosphate. The ϵ -amino group of hood residue Lys26B extends across orotate to form a hydrogen bond to the α -phosphate. The backbone nitrogens of Tyr72B and Lys73B interact with β -phosphate. All of the interactions of the pyrophosphoryl group are with residues that have moved from their positions in other structures.

The PRPP binding seen in subunit B of PDB entry 1LH0 is strikingly different from that in the previous substrate complex, PDB entry 1OPR, which is symmetric (Figure 7). In PDB entry 1OPR, the 5-phosphate of PRPP does not interact closely with the phosphate binding pocket in subunit A (3.0–4.1 Å NH–O distances), nor is it so close to O4' (4.9 Å). Residues 128–132 have higher (28 – 57 Å² vs an average of 30 Å²) *B* factors in this subunit. The side chain of Thr128 makes a 2.6 Å hydrogen bond with a 5-phosphate oxygen, replacing one to the orotate carboxylate in subunit B, and no hydrogen bonding interaction

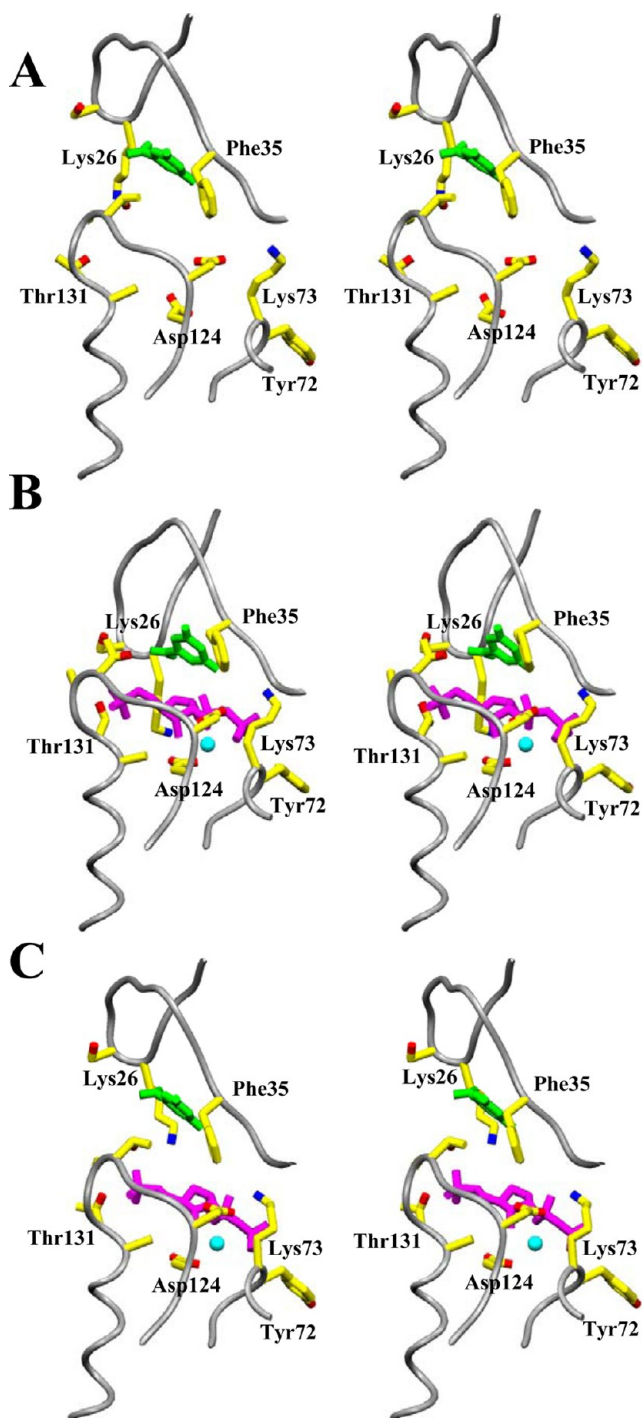


Figure 7. Stereoviews comparing the substrate binding area of PRPP complexes. The backbone is shown in worm format in gray, and selected side chains (yellow), orotate (green), PRPP (red), and Mg^{2+} (light blue) are shown as balls and sticks. (A) Subunit A, containing only orotate, of the current complex (PDB entry 1LH0). (B) Subunit B of the current loop-closed E-MgPRPP-orotate complex (PDB entry 1LH0). (C) Corresponding area of the previous loop-open E-MgPRPP-orotate complex (PDB entry 1OPR²¹), resembling the more open subunit A of PDB entry 1LH0.

with Asp125A (4.7 Å) is present in subunit A. The pyrophosphoryl group makes remarkably different contacts in the open subunit. Hydrogen bonds to Lys100A are absent; only a single hydrogen bond is formed to Arg99B, and hydrogen bonds to catalytic loop residues Lys103B and His105B are not

present. The interactions of main chain nitrogens of Tyr72A (2.7 Å) and Lys73A (2.3 Å) with the β -phosphate are preserved.

Active Site Water Molecules. A major function of loop closure in Type I PRTases is to exclude solvent from the developing transition state.^{10,21,23} However, the active site of subunit B contains a total of 10 water molecules, with B factors ranging from 15.5 to 51.2 Å², compared to the overall B factor of 29 Å² for atoms of the protein. Because OMP synthase is very effective in avoiding alternative hydrolysis reactions of PRPP and OMP (C. Grubmeyer, unpublished observations), these water molecules are clearly restrained from reacting with the developing transition state.

DISCUSSION

The key finding of our work is that *S. typhimurium* OMP synthase can exist in a conformer with its catalytic loop in a highly structured β -form that sequesters the active site from bulk solvent and contributes key residues to the active site. Unlike HGPRTase, the OMP synthase loop moves across the subunit interface to affect catalysis in the adjacent site. Although this loop-down conformer had been anticipated,^{22–24,26,40} its direct observation here permits much fuller interpretation of the mechanistic roles of specific residues. Remarkably, movement of the loop from subunit A is accompanied by a dramatic tightening of the structure of subunit B, with the formation of many new hydrogen bonds.

The current structure results from cocrystallization. The complex, like that published previously (PDB entry 1OPR²¹), contains orotate, PRPP, and Mg^{2+} with no observational OMP or PP_i. Figure 7 presents a comparison of the loop-open, orotate-containing active site of subunit A of PDB entry 1LH0 (Figure 7A) versus the loop-closed orotate- and MgPRPP-containing active site of subunit B (Figure 7B). Figure 7C shows the structure of PDB entry 1OPR, with an active site structure resembling that of subunit A of PDB entry 1LH0. The previous complex (PDB entry 1OPR) was the result of a crystal soaking procedure, and crystal lattice constraints or crystallization components may have prevented the achievement of the loop-closed conformation. In solution, the on-enzyme equilibrium between E·MgPRPP·orotate and E·OMP·PP_i Michaelis complexes (K_{int} is 1:2, with rapid (300 s^{−1}) interconversion.²⁷ The selective stabilization of one form may also be linked to barriers imposed by the crystal lattice. An alternative is that crystallization has captured a nonproductive complex. However, the nearly ideal positions of catalytic residues and substrates suggest a productive form is being viewed. PRPP is an unstable molecule, susceptible to base-catalyzed elimination of β -phosphate following intramolecular attack of O2' on the α -phosphate.⁴¹ The intact PRPP in the complex may originate in part from the large molar excess present during crystal growth and because the cryoprotectant solution contained fresh PRPP. However, unpublished studies (C. Grubmeyer's laboratory) have shown that OMP synthase in fact protects bound PRPP in binary complexes from base-catalyzed degradation, and this protection may be enhanced in a completely closed complex.

The rearrangement observed in subunit B of PDB entry 1LH0 versus PDB entry 1OPR, and the striking asymmetry of the dimer in PDB entry 1LH0, can be rationalized on the basis of interactions in the individual subunits. The presence of PRPP sets up a competition for hydrogen bonds donated by Lys100 and Arg99. As subunit B captures the catalytic loop of

subunit A, Lys100A is pulled away from its position in the PRPP binding site of subunit A. In subunit B, the correct positioning of Lys100B and Arg99A allows PRPP movement and permits the catalytic loop of subunit A to deploy over subunit B, promoting the interaction of Lys103A and His105A with bound PRPP. The position of PRPP in PDB entry 1OPR remains closer to the subunit interface, and both catalytic loops, which are being pulled by the interaction of Lys100 with PRPP, remain open and disordered. The failure of the hood of subunit A of PDB entry 1LH0 to move toward the phosphate binding loop appears to result from the lack of stabilizing interactions with the catalytic loop of subunit B, rather than any obvious steric conflict. It should be noted that the position of catalytic loop B is not represented in the electron density, and thus, it may not be in the fully solvent-extended conformation seen previously.²¹ The structural asymmetry seen here does raise the very interesting possibility that enzyme function is also asymmetric. Related observations by the groups of McClard and Witte on the kinetics, binding, and structure of the yeast enzyme, and of the bacterial complex that we presented in PDB entry 1LH0, have led to a detailed mechanism for alternating sites cooperativity.^{25,26}

The functional correlates of the structural asymmetry seen here remain to be established. Previous chemical modification kinetics and stoichiometries⁴⁰ and steady state⁴² and pre-steady state²⁷ kinetic studies have provided no evidence of functional kinetic cooperativity by the *S. typhimurium* enzyme, although the McClard group has observed such behavior for the yeast enzyme.²⁶ NMR and partial proteolysis studies of binary complexes identified forms of the *S. typhimurium* enzyme with both catalytic loops in a closed position, and although the structure of the loop was not characterized in that work, heterogeneity might have been observed through chemical shift exchange. In addition, binding studies with binary complexes have shown that each of the four substrates for the enzyme can bind to two sites per dimer with a single K_D .²⁷ Net reverse catalysis by OMP synthase involves rapid chemistry (100 s^{-1}) and slower PRPP release, which requires catalytic loop opening at 400 s^{-1} , and partitioning of the open complex between loop closure (12000 s^{-1}) and PRPP release (2200 s^{-1}).²⁸ This indicates a delicate poise between forces serving to stabilize the loop-closed structure (including the many bonds described here) and those tending to promote its return to a solvent-extended position. These may include hydration of the loop and the active site itself. It is quite possible that interactions between the two catalytic sites may help subunit B release product as subunit A fills and recaptures the loop of subunit B. This could produce the flattening of the free energy profile that enhances enzyme efficiency.

Comparisons to Other Ribosyltransferases. Improving knowledge of protein and transition state structures of ribosyltransferases has resulted in a general proposal for their action⁴³ in which oxocarbenium-like transition states are stabilized by the 5'-oxygen and a second oxygen, here the carboxyl of orotate, and that reaction requires migration of the developing oxocarbenium entity (C1'-O4') in the reaction trajectory. Here, that movement appears to be $\sim 1.8\text{ \AA}$ (the 4.8 \AA N-C-O axis, minus 3.0 \AA for the N1-C1' and C1'-OPP covalent bonds), although a Michaelis-like E·OMP·MgPP_i complex will help define this motion better. OMP synthase provides a paradigm in this group because its reaction is freely reversible and a transition state structure is known.^{36,37}

■ ASSOCIATED CONTENT

Accession Codes

Coordinates for this structure have been deposited in the Protein Data Bank (PDB) as entry 1LH0.

■ AUTHOR INFORMATION

Corresponding Author

*C.G.: telephone, (215) 707-4495; e-mail, ctg@temple.edu. S.C.A.: telephone, (718) 430-2746; e-mail, almo@aecom.yu.edu.

Funding

This research was supported by National Institutes of Health Grant GM48623 to C.G. and S.C.A.

Notes

The authors declare no competing financial interest.

■ ACKNOWLEDGMENTS

We thank Bradley Bizzle for preparation of the enzyme and Eric Barr for assistance with ChemDraw. C.G. thanks Drs. Richard Furneaux and Peter Tyler (Industrial Research Ltd., Wellington, New Zealand) for pointing out the potential role of orotate in stabilizing the oxocarbenium character of the transition state.

■ ABBREVIATIONS

OMP synthase, orotate phosphoribosyltransferase; PRTase, phosphoribosyltransferase; HGPRTase, hypoxanthine-guanine PRTase; OMP, orotidine 5'-phosphate; PRPP, D-5-phosphoribosyl α -1-pyrophosphate; GPAT, glutamine PRPP amidotransferase; rmsd, root-mean-square deviation. We use the prime symbol to denote atoms of the ribosyl ring of PRPP or OMP.

■ REFERENCES

- (1) Jones, M. E. (1980) Pyrimidine nucleotide biosynthesis in animals: Genes, enzymes, and regulation of UMP biosynthesis. *Annu. Rev. Biochem.* 49, 253–279.
- (2) Suttle, D. P., Becroft, D. M. O., and Webster, D. R. (1989) Disorders of Pyrimidine Metabolism. In *The Metabolic Basis of Inherited Disease* (Scriver, C. R., Beaudet, A. L., Sly, W. S., and Valle, D., Eds.) 6th ed., pp 1095–1126, McGraw-Hill, New York.
- (3) Musick, W. D. (1981) Structural features of the phosphoribosyltransferases and their relationship to the human deficiency disorders of purine and pyrimidine metabolism. *CRC Crit. Rev. Biochem.* 11, 1–34.
- (4) Smith, J. L. (1999) Forming and inhibiting PRT active sites. *Nat. Struct. Biol.* 6, 502–504.
- (5) Hove-Jensen, B., Harlow, K. W., King, C. J., and Switzer, R. L. (1986) Phosphoribosylpyrophosphate synthetase of *Escherichia coli*. Properties of the purified enzyme and primary structure of the prs gene. *J. Biol. Chem.* 261, 6765–6771.
- (6) Eriksen, T. A., Kadziola, A., Bentsen, A. K., Harlow, K. W., and Larsen, S. (2000) Structural basis for the function of *Bacillus subtilis* phosphoribosylpyrophosphate synthetase. *Nat. Struct. Biol.* 7, 303–308.
- (7) Eads, J. C., Ozturk, D., Wexler, T. B., Grubmeyer, C., and Sacchettini, J. C. (1997) A new function for a common fold: The crystal structure of quinolinic acid phosphoribosyltransferase. *Structure* 5, 47–58.
- (8) Shin, D. H., Oganessian, N., Jancarik, J., Yokota, H., Kim, R., and Kim, S. H. (2005) Crystal structure of a nicotinate phosphoribosyltransferase from *Thermoplasma acidophilum*. *J. Biol. Chem.* 280, 18326–18335.
- (9) Wang, T., Zhang, X., Bheda, P., Revollo, J. R., Imai, S., and Wolberger, C. (2006) Structure of Namp/PBEF/visfatin, a

mammalian NAD⁺ biosynthetic enzyme. *Nat. Struct. Mol. Biol.* 13, 661–662.

(10) Eads, J. C., Scapin, G., Xu, Y., Grubmeyer, C., and Sacchettini, J. C. (1994) The crystal structure of human hypoxanthine-guanine phosphoribosyltransferase with bound GMP. *Cell* 78, 944–948.

(11) Vos, S., Parry, R. J., Burns, M. R., deJersey, J., and Martin, J. L. (1998) Structures of free and complexed forms of *Escherichia coli* xanthine-guanine phosphoribosyltransferase. *J. Mol. Biol.* 282, 875–889.

(12) Munagala, N., Basus, V. J., and Wang, C. C. (2001) Role of the flexible loop of hypoxanthine-guanine-xanthine phosphoribosyltransferase from *Tritrichomonas foetus* in enzyme catalysis. *Biochemistry* 40, 4303–4011.

(13) Shi, W., Li, C. M., Tyler, P. C., Furneaux, R. H., Cahill, S. M., Girvin, M. E., Grubmeyer, C., Schramm, V. L., and Almo, S. C. (1999) The 2.0 Å structure of malarial purine phosphoribosyltransferase in complex with a transition-state analogue inhibitor. *Biochemistry* 38, 9872–9880.

(14) Heroux, A., White, E. L., Ross, L. J., Davis, R. L., and Borhani, D. W. (1999) Crystal structure of *Toxoplasma gondii* hypoxanthine-guanine phosphoribosyltransferase with XMP, pyrophosphate, and two Mg²⁺ ions bound: Insights into the catalytic mechanism. *Biochemistry* 38, 14495–14506.

(15) Balendiran, G. K., Molina, J. A., Xu, Y., Torres-Martinez, J., Stevens, R., Focia, P. J., Eakin, A. E., Sacchettini, J. C., and Craig, S. P. (1999) Ternary complex structure of human HGPRTase, PRPP, Mg²⁺, and the inhibitor HPP reveals the involvement of the flexible loop in substrate binding. *Protein Sci.* 8, 1023–1031.

(16) Heroux, A., White, E. L., Ross, L. J., and Borhani, D. W. (1999) Crystal structures of the *Toxoplasma gondii* hypoxanthine-guanine phosphoribosyltransferase-GMP and -IMP complexes: Comparison of purine binding interactions with the XMP complex. *Biochemistry* 38, 14485–14494.

(17) Shi, W., Li, C. M., Tyler, P. C., Furneaux, R. H., Grubmeyer, C., Schramm, V. L., and Almo, S. C. (1999) The 2.0 Å structure of human hypoxanthine-guanine phosphoribosyltransferase in complex with a transition-state analog inhibitor. *Nat. Struct. Biol.* 6, 588–596.

(18) Xu, Y., Eads, J. C., Sacchettini, J. C., and Grubmeyer, C. (1997) Kinetic mechanism of human hypoxanthine-guanine phosphoribosyltransferase: Rapid phosphoribosyl transfer chemistry. *Biochemistry* 36, 3700–3712.

(19) Chen, S., Burgner, J. W., Krahn, J. M., Smith, J. L., and Zalkin, H. (1999) Tryptophan fluorescence monitors multiple conformational changes required for glutamine phosphoribosylpyrophosphate amidotransferase interdomain signaling and catalysis. *Biochemistry* 38, 11659–11669.

(20) Scapin, G., Grubmeyer, C., and Sacchettini, J. C. (1994) Crystal structure of orotate phosphoribosyltransferase. *Biochemistry* 33, 1287–1294.

(21) Scapin, G., Ozturk, D. H., Grubmeyer, C., and Sacchettini, J. C. (1995) The crystal structure of the orotate phosphoribosyltransferase complexed with orotate and α -D-5-phosphoribosyl-1-pyrophosphate. *Biochemistry* 34, 10744–10754.

(22) Ozturk, D. H., Dorfman, R. H., Scapin, G., Sacchettini, J. C., and Grubmeyer, C. (1995) Locations and functional roles of conserved lysine residues in *Salmonella typhimurium* orotate phosphoribosyltransferase. *Biochemistry* 34, 10755–10763.

(23) Ozturk, D. H., Dorfman, R. H., Scapin, G., Sacchettini, J. C., and Grubmeyer, C. (1995) Structure and function of *Salmonella typhimurium* orotate phosphoribosyltransferase: Protein complementation reveals shared active sites. *Biochemistry* 34, 10764–10770.

(24) Henriksen, A., Aghajari, N., Jensen, K. F., and Gajhede, M. (1996) A flexible loop at the dimer interface is a part of the active site of the adjacent monomer of *Escherichia coli* orotate phosphoribosyltransferase. *Biochemistry* 35, 3803–3809.

(25) González-Segura, L., Witte, J. F., McClard, R. W., and Hurley, T. D. (2007) Ternary complex formation and induced asymmetry in orotate phosphoribosyltransferase. *Biochemistry* 46, 14075–14086.

(26) McClard, R. W., Holets, E. A., MacKinnon, A. L., and Witte, J. (2006) Half-of-sites binding of orotidine 5'-phosphate and α -D-5-phosphorylribose 1-diphosphate to orotate phosphoribosyltransferase from *Saccharomyces cerevisiae* supports a novel variant of the Theorell-Chance mechanism with alternating site catalysis. *Biochemistry* 45, 5330–5342.

(27) Wang, G. P., Lundegaard, C., Jensen, K. F., and Grubmeyer, C. (1999) Kinetic mechanism of OMP synthase: A slow physical step following group transfer limits catalytic rate. *Biochemistry* 38, 275–283.

(28) Wang, G. P., Cahill, S. M., Liu, X., Girvin, M. E., and Grubmeyer, C. (1999) Motional dynamics of the catalytic loop in OMP synthase. *Biochemistry* 38, 284–295.

(29) Otwinowski, Z., and Minor, W. (1997) Processing of X-ray diffraction data collected in oscillation mode. *Methods Enzymol.* 276, 307–326.

(30) Navaza, J. (1994) AMoRe: An automated package for molecular replacement. *Acta Crystallogr. A* 50, 157–163.

(31) Brunger, A. T. (1992) X-PLOR, version 3.1, Yale University Press, New Haven, CT.

(32) Jones, T. A., Zou, J. Y., Cowan, S. W., and Kjeldgaard, M. (1991) Improved methods for building protein models in electron density maps and the location of errors in these models. *Acta Crystallogr. A* 47, 110–119.

(33) Kleywegt, G. J., and Jones, T. A. (1998) Databases in Protein Crystallography. *Acta Crystallogr. D* 54, 1119–1131.

(34) Heroux, A., White, E. L., Ross, L. J., Kuzin, A. P., and Borhani, D. W. (2000) Substrate deformation in a hypoxanthine-guanine phosphoribosyltransferase ternary complex: The structural basis for catalysis. *Structure* 8, 1309–1318.

(35) Laskowski, R. A., MacArthur, M. W., Moss, D. S., and Thornton, J. M. (1993) PROCHECK: A program to check the stereochemical quality of protein structures. *J. Appl. Crystallogr.* 26, 283–291.

(36) Tao, W., Grubmeyer, C., and Blanchard, J. S. (1996) Transition state structure of *Salmonella typhimurium* orotate phosphoribosyltransferase. *Biochemistry* 35, 14–21.

(37) Zhang, Y., Luo, M., and Schramm, V. L. (2009) Transition states of *Plasmodium falciparum* and human orotate phosphoribosyltransferases. *J. Am. Chem. Soc.* 131, 4685–4694.

(38) Niedzwicki, J. G., Iltzsch, M. H., el Kouni, M. H., and Cha, S. (1984) Structure-activity relationship of pyrimidine base analogs as ligands of orotate phosphoribosyltransferase. *Biochem. Pharmacol.* 33, 2383–2395.

(39) Krahn, J. M., Kim, J. H., Burns, M. R., Parry, R. J., Zalkin, H., and Smith, J. H. (1997) Coupled formation of an amidotransferase interdomain ammonia channel and a phosphoribosyltransferase active site. *Biochemistry* 36, 11061–11068.

(40) Grubmeyer, C., Segura, E., and Dorfman, R. (1993) Active site lysines in orotate phosphoribosyltransferase. *J. Biol. Chem.* 268, 20299–20304.

(41) Khorana, H. G., Fernandes, J. F., and Kornberg, A. (1958) Pyrophosphorylation of ribose 5-phosphate in the enzymatic synthesis of 5-phosphorylribose 1-pyrophosphate. *J. Biol. Chem.* 230, 941–948.

(42) Bhatia, M., Vinitsky, A., and Grubmeyer, C. (1990) Kinetic mechanism of orotate phosphoribosyltransferase from *Salmonella typhimurium*. *Biochemistry* 29, 10480–10487.

(43) Fedorov, A., Shi, W., Kicska, G., Fedorov, E., Tyler, P. C., Furneaux, R. H., Hanson, J. C., Gainsford, G. J., Larese, J. Z., Schramm, V. L., and Almo, S. C. (2001) Transition state structure of purine nucleoside phosphorylase and principles of atomic motion in enzymatic catalysis. *Biochemistry* 40, 853–860.